Langmuir

Article

pubs.acs.org/Langmuir

CO_2 Electroreduction at Bare and Cu-Decorated Pd Pseudomorphic Layers: Catalyst Tuning by Controlled and Indirect Supporting onto Au(111)

Aneta Januszewska,[†] Rafal Jurczakowski,*[,†] and Pawel J. Kulesza*[,‡]

[†]Faculty of Chemistry, Biological and Chemical Research Centre, University of Warsaw, Zwirki i Wigury 101, PL-02-093 Warsaw, Poland

[‡]Faculty of Chemistry, University of Warsaw, ul Pasteura 1, 02-093 Warsaw, Poland

Supporting Information

ABSTRACT: We report here the results of electrochemical studies on CO_2 electroreduction at multilayered catalyst composed of the monatomic layer of copper covering palladium overlayers (0.8−10 monolayers) deposited on the well-defined Au(111) surface. These multilayered systems were obtained by successive underpotential deposition steps: Pd on Au(111) as well as Cu on Pd/Au(111). Low index orientation of Au substrate was chosen to compare Pd overlayers with bulk Pd(111), which is known to reduce CO_2 to CO adsorbates in acidic solutions. The process of CO_2 electroreduction was studied by using classical transient electrochemical methods. Catalytic activity of bare Pd layers was investigated in acidic and neutral solutions. In the latter case, much higher activity of Pd overlayers was observed. The results showed that the palladium layer thickness significantly changed the catalytic activities of both bare Pd overlayers and the one Cu monolayer covered electrodes toward CO_2 electroreduction. Results show that catalytic activity can be finely tuned by using the multilayered near-surface-alloy approach.

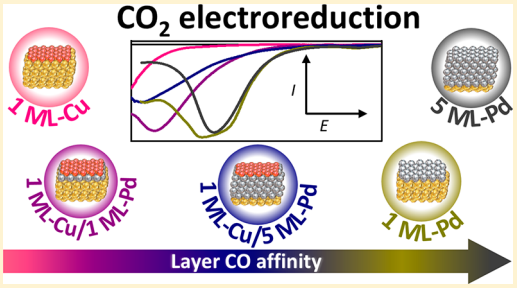

1. INTRODUCTION

Atmospheric carbon dioxide levels have risen rapidly over the past few decades. Electrochemical conversion of carbon dioxide into eligible fuels has potential as the technology that may diminish serious environmental problems. Carbon dioxide reduction on metallic surfaces has recently become one of the main topics in electrocatalytic studies. The CO_2 electroreduction to hydrocarbons is a complex process that usually involves adsorbed carbon monoxide as an intermediate.[1] Hence, the overall electroreduction path is determined, to a large extent, by the catalyst's surface affinity to carbon monoxide; the strongly bound CO inhibits further reduction[1] while the weakly bound CO easily desorbs and becomes the final product. Recently, it has been shown by means of theoretical model based on density functional theory that CO is produced through the adsorbed intermediates $COOH_{(ads)}$ and $CO_{(ads)}$.[2] Surface affinity to CO can be controlled by changing the lattice constant of the heterogeneous metallic catalyst.[3] This effect can be achieved by deposition of the metal monatomic layers on foreign metallic surfaces. Deposition of metal overlayers on well-defined surfaces and the resulting systems' catalytic activities become a subject of numerous electrocatalytic and surface studies.[4−7] Geometric and electronic modifications of pseudomorphic Pd overlayers affect both CO and hydrogen adsorption.[8,9] Obviously deposited monolayers differ in the dependence of the surface defects density.[8,10] Differences occur mainly at the oxide region, CO-stripping experiments and also at Pd UPD peaks during deposition.[8,11] However, the degree of modifications of catalytic properties of such surfaces is rather limited since the lattice constant characteristic for bulk material is promptly reconstructed with consecutive overlayers, generally, as early as in the second layer.[12−16] The chemical influence of the background material is also much weaker for thicker deposits. Recently, it has been shown that the unique catalytic properties can be achieved by preparation of near-surface alloys (NSA's).[17] For metal chalcogen systems, the possibility of preparation of multilayered NSAs by sequential UPD strategies has also been demonstrated.[18]

Carbon dioxide electroreduction on thin palladium films deposited on polycrystalline gold electrode was recently reported by Obradovic et al.[16] The authors reported higher activity toward CO_2 reduction on 4 monolayers (ML) of palladium than on Pd black. Carbon dioxide electroreduction was also studied at Cu/Pt(111) and Cu/Pt(211).[19] These surfaces were characterized by higher total current densities with respect to pure copper; however, the current efficiency of this process was rather low since the current related to hydrogen evolution reaction dominated in the overall current density.

Received: June 26, 2014
Revised: September 15, 2014
Published: October 28, 2014

Herein we report, for the first time, the results of CO_2 electroreduction on model multilayered palladium catalysts composed of the monatomic layer of copper covering palladium overlayers (0.8−10 ML) deposited on the well-defined Au(111) surface. These multilayers were obtained by successive underpotential deposition of Pd on Au(111) and the deposition of Cu on Pd/Au(111). Low index orientation of Au substrate was chosen to compare Pd overlayers with bulk Pd(111) electrode, which is known to reduce CO_2 to adsorbed CO in acidic solutions.[4] The gold electrode itself has weak affinity to CO, and therefore, the main product of CO_2 electroreduction is gaseous CO.[20] Here, the process of CO_2 electroreduction was studied in acidic and neutral solutions by using classical transient electrochemical methods. Our results clearly demonstrate that the Pd-layer thickness (studied within the range 0.8−10 ML) significantly changes the surface catalytic activity of palladium toward CO_2 electroreduction. Interestingly, multilayered films covered with the copper monolayer largely reflect the properties of palladium deposits existing under the Cu surface. What is even more important, the fine catalyst tuning by using the multilayered NSA approach is feasible.

2. EXPERIMENTAL SECTION

2.1. Electrodes. Counter electrode was gold foil. The reference electrode was Hg|Hg_2SO_4|0.1 M H_2SO_4 and Hg|Hg_2SO_4|sat. K_2SO_4 in acidic and neutral solution, respectively. In the acidic solutions, the mercury sulfate electrode potentials were found to be 0.718 and 0.720 V (vs RHE) in sulfuric acid and perchloric acid solutions, respectively. In 0.1 M $KHCO_3$, the reference electrode potential was 1.14 V against RHE. The pH's of pure 0.1 M potassium bicarbonate and CO_2 saturated solution were 8.9 and 6.8, respectively. The potential of the reference electrode in the CO_2-saturated solution was calculated upon consideration of the solution pH, and it was found to be 1.012 V.

2.2. Catalysts Preparation. Palladium overlayers were deposited on monocrystalline Au(111) in a form of the cylindrical disk of 6 mm diameter (MaTeck). Before deposition, the gold electrode was electrochemically polished in a galvanostatic step performed in 0.1 M H_2SO_4 through application of 1 mA cm^{-2} current for 300 s. Oxide layers were dissolved in 1 M HCl, and the electrode was thoroughly rinsed with Milli-Q deionized water. Next, gold Au(111) electrode was annealed in a hydrogen flame and cooled in the electrochemical cell above the electrolyte deaerated in the stream of argon. Prior to deposition, the quality of the Au(111) substrate was verified with cyclic voltammetry in pure acid. Palladium deposits were obtained from bath containing 0.1 M H_2SO_4 and 1 mM H_2PdCl_4. A detailed method for Pd layer depositions can be found elsewhere.[9,21] In brief, underpotential monolayer of Pd was deposited by scanning potential at 0.1 mV s^{-1} from 0.918 to 0.828 V vs RHE. The final potential was held for 300 s until the flowing current dropped to zero. The Pd monolayer type UPD deposits are further denoted as 1 ML-Pd; however, the typical Pd coverage was ∼0.8 ML as deduced from the deposition charges. To obtain 2−10 layers, the potential was scanned from 0.918 to 0.723 V vs RHE and held until the total charge reached the value characteristic of a given thickness. This deposition process is known to result in the formation of defect-rich dendric shapes. Consequently, 5 monolayers (further denoted as 5-ML) were nonsmooth layers but simply palladium structures deposited with charge equivalent to five monolayers. Each layer on the electrode was deposited on a clean and renewed electrode surface. Multilayered catalysts were obtained by the Cu-UPD approach performed onto palladium overlayers in 0.1 M H_2SO_4 + 0.5 mM $CuSO_4$ solution. The Cu coverage was estimated to be ∼0.65 ML, but for simplicity, it is further denoted as 1 ML-Cu.

Palladium layers were removed from Au(111) surface by immersing the electrode in a solution containing 50 mL of HNO_3 + 100 μL of HCl for 2 s followed by thorough rinsing with deionized water.

2.3. CO-Stripping Experiments. CO was adsorbed on the electrode surface under potentiostatic conditions following the CO injection into the cell as a rule for 10 min to achieve the surface saturation coverage. Adsorption of CO was achieved on the electrode surface at different potentials, namely within the double layer, HUPD and HOPD regions. In the final step, the CO was removed by purging argon through solution for 15 min, and cyclic voltammograms were registered.

3. RESULTS AND DISCUSSION

3.1. Characterization of Pd/Au(111) Overlayers in Acidic Solutions. Both the morphology of the palladium deposits and their activity toward carbon dioxide reduction are highly influenced by the surface defect density of the monocrystalline background electrode.[8] Hence, the gold Au(111) substrate was examined by using cyclic voltammetry in acidic environment before each deposition. The exemplary result obtained in 0.1 M sulfuric acid solution is shown in Figure 1 (gray dashed curve, right axis); this result is in

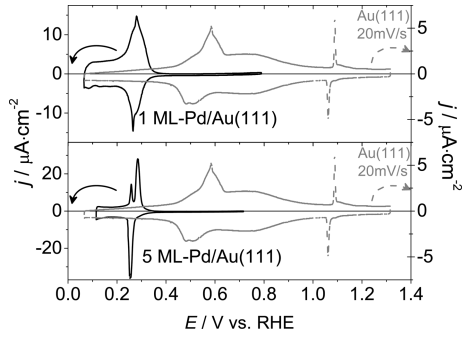

Figure 1. Cyclic voltammograms of 1 ML (top) and 5 ML (bottom) Pd/Au(111) electrodes in 0.1 M H_2SO_4. Scan rate: 5 mV s^{-1} (black continuous lines, left axis). For the sake of comparison, the voltammograms of Au(111) substrate was also included. Scan rate: 20 mV s^{-1} (gray dashed lines, right axis).

agreement with previously reported results obtained for the defect-free Au(111) surfaces.[8,22,23] Freshly deposited palladium layers were also initially tested in 0.1 M sulfuric or/and perchloric acid solution before performing experiments in potassium bicarbonate solution. Figure 1 (black solid lines) shows cyclic voltammograms recorded in this study for 1 ML-Pd/Au(111) (top) and 5 ML-Pd/Au(111) (bottom) in 0.1 M H_2SO_4 at the scan rate of 5 mV s^{-1}. The voltammetric responses are virtually identical to those reported earlier in the literature.[14,24] On 1 ML-Pd/Au(111), the hydrogen adsorption/desorption occurs at 0.272 V vs RHE. The separation of the hydrogen adsorption/desorption peaks is related to the slower reaction kinetics on the Pd/Au(111) surface in comparison to bulk palladium. The peak broadening reflects contributions from remaining palladium islands, which have not coalesced during cycling,[24] and at more positive potentials, contributions from (bi)sulfate adsorption/desorption also appear. Total hydrogen adsorption charge calculated within the potential range 0.35−0.1 V is 170 μC cm^{-2}. Similar results were obtained in 0.1 M H_2SO_4 for 1 ML by Duncan et al.[24] This charge corresponds to the surface coverage of ∼0.8 ML.

For 5 ML-Pd/Au(111) (Figure 1 (bottom)) the total hydrogen adsorption charge is Q_H = 220 μC cm^{-2}. The anodic peak at 0.285 V is related to both the hydrogen desorption and the (bi)sulfate adsorption. The first Pd layer is not entirely covered and the deposit still exposes monatomic underlayer.[25]

dx.doi.org/10.1021/la5025247 | Langmuir 2014, 30, 14314−14321

In conclusion, the present cyclic voltammetric responses obtained in acidic solutions (when compared to literature data) have confirmed the good quality of deposited Pd layers.

3.2. Characterization of Pd/Au(111) Overlayers in $KHCO_3$ Solution. In alkaline media, pseudomorphic Pd layers have been studied by Marin et al. in NaOH solution[26] while voltammetric behavior in (bi)carbonate ions containing solution has not been reported. Therefore, it was necessary to investigate the well-defined Pd monolayers in neutral (CO_2-saturated) and basic 0.1 M $KHCO_3$ solutions. Cyclic voltammograms of 1 ML-Pd/Au(111) in pure 0.1 M $KHCO_3$ (pH = 8.9) are displayed in Figure 2. First, the anodic potential

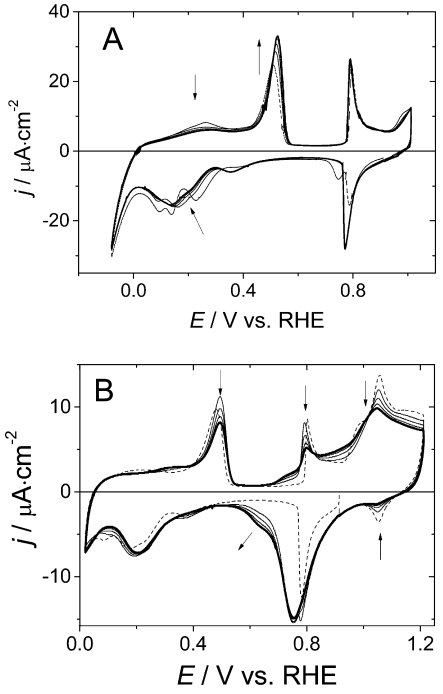

Figure 2. (A) Cyclic voltammograms recorded at 20 mV s^{-1} for 1 ML-Pd/Au(111) with anodic limit 1.0 V. (B) Cyclic voltammogram with anodic limit 1.2 V and scan rate 10 mV s^{-1}, 0.1 M $KHCO_3$.

limit has been set to 1.0 V vs RHE (Figure 2A). The hydrogen adsorption currents occur at potentials within the range 0–0.55 V vs RHE. Peak separation between the two main hydrogen adsorption/desorption peaks is 391 mV in 0.1 M $KHCO_3$ while, in the acidic media, the value as low as 39 mV was observed at the same scan rate (v = 20 mV s^{-1}). This effect reflects much slower kinetics of the hydrogen absorption/desorption processes at higher pH. The total charge of adsorbed hydrogen in pure 0.1 M $KHCO_3$ solution, Q_H = 162 μC cm^{-2}, is only slightly smaller than that measured in 0.1 M H_2SO_4 solution, where Q_H = 170 μC cm^{-2} was observed. Another important difference (in comparison to acidic solutions) is a pair of sharp peaks visible at 0.78 V. The charge related to those peaks is Q = 58.5 μC cm^{-2}; their origin is not clear. However, the reversible character and small peak separation, 23 mV, suggest a fast process of the formation of a long-range ordered anion adlayer on the (111) terraces. A similar pair of peaks was observed in the case of sulfate adsorption on Pd(111) as reported by Hara et al.[11] When pH of the solution is changed from 8.9 to 6.8 (after CO_2 saturation), these peaks shift by 233 mV toward higher potentials. Taking into account acid–base equilibria in (bi)carbonate solutions,[27] this potential shift correspond to the slope ~110 mV per decade of CO_3^{2-} and OH^- ions concentration. This result may suggest concerted adsorption of CO_3^{2-} and OH^- ions as it was suggested for Pt(110) electrode in sodium bicarbonate solutions.[28]

Figure 2B shows the oxidation of 1 ML-Pd/Au(111) electrode. In the first cycle, a sharp anodic peak at 1.05 V can be observed for the well-ordered Pd layer; subsequently, the reduction of palladium oxides occurs in a form of a single cathodic peak with the maximum at 0.75 V. The very first cycle shows a pair of sharp oxidation/reduction peaks at 1.05 V related to the oxidation of the well-ordered Pd(111) surface. These peaks decrease upon potential cycling while a new pair of peaks appears at less positive potentials, and a stable voltammetric behavior response is obtained after the third cycle. This new pair of peaks can be ascribed to the oxidation of surface defects by analogy to similar results observed in acidic solution.[8] The charges for oxide formation Q = 387 μC cm^{-2} and reduction Q = 336 μC cm^{-2} are nearly balanced, thus suggesting that dissolution of the Pd layer is generally less pronounced in $KHCO_3$ solutions relative to acidic solutions.[10,11]

It should be noticed that the pair of peaks at 0.78 V (Figure 2B) markedly diminish with each cycle. In the case of (bi)sulfate adsorption, similar behavior was observed for Pd(111) surface before and after oxidation in 0.1 M H_2SO_4 as reported by Hara et al. and El-Aziz et al.[8,11] This effect is related to surface phase transition and the formation of disordered layer, at which the long-range ordered anions adlayer cannot be formed.

3.3. Carbon Dioxide Electroreduction at Pd/Au(111) Overlayers. Carbon dioxide electroreduction was studied in bicarbonate buffer (0.1 M $KHCO_3$ saturated with CO_2, pH = 6.8) first in the potential range where the hydrogen evolution does not take place in order to verify whether it is possible to reduce CO_2 in the HUPD region. Figure 3 shows cyclic

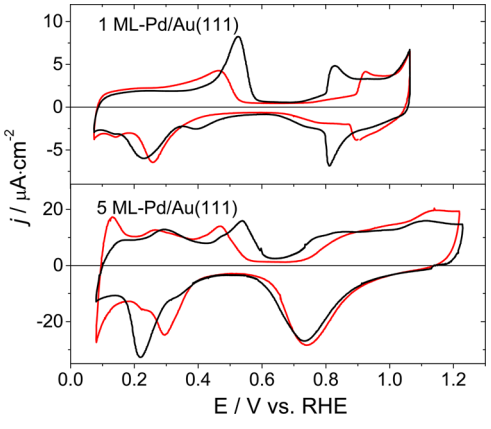

Figure 3. Cyclic voltammograms of (top) 1 ML-Pd/Au(111) and (bottom) 5 ML-Pd/Au(111) in pure (black lines) and CO_2-saturated 0.1 M $KHCO_3$ solution (red lines). Scan rate: 20 mV s^{-1}.

voltammograms registered for 1 and 5 ML Pd/Au(111) in the presence (red lines) and in the absence (black lines) of CO_2 in 0.1 M $KHCO_3$. In the case of 5 ML Pd, the HUPD region is typical for basic solutions and hydrogen peaks are similar to peaks at 10 ML-Pd/Au(111) in 0.1 M NaOH reported by Martin et al.[26] The anodic peak at 0.538 V is ascribed to hydrogen desorption from the Pd steps, and the peak at 0.294

dx.doi.org/10.1021/la5025247 | Langmuir 2014, 30, 14314–14321

V refers to hydrogen desorption from the Pd terraces. In the presence of CO_2 in the solution, the hydrogen charges related to the hydrogen adsorption decrease to Q_H = 125 μC cm^{-2} for 1 ML-Pd/Au(111) and to Q_H = 145 μC cm^{-2} for 5 ML-Pd/Au(111). This effect was ascribed to a weak CO_2 adsorption. Since no excessive current was observed in the oxide region, the CO_2 electroreduction and the formation of poisonous intermediates in this potential range seem to be unlikely. The voltammetric shape depends on the pH of the solution in both hydrogen and oxide regions. It is interesting to note that Pd oxide formation begins at higher potentials for both 1 and 5 Pd ML in CO_2-saturated solutions.

Figure 4 shows cyclic voltammograms recorded for Pd/Au(111) layers in a wider potential range. In the presence of

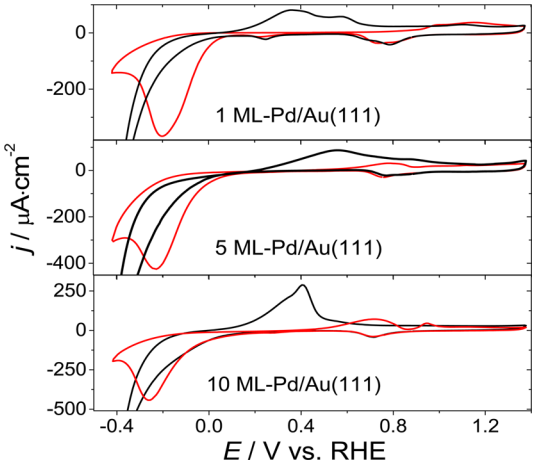

Figure 4. Comparison of 1 ML-Pd/Au(111), 5 ML-Pd/Au(111), and 10 ML-Pd/Au(111) in pure (black lines) and CO_2-saturated (red lines) 0.1 M $KHCO_3$ solution. Scan rate: 20 mV s^{-1}.

CO_2 in the solution (red lines), a broad cathodic peak appears in all voltammograms below 0 V vs RHE. It should be noticed that this peak is absent in the CO_2-free solution (black lines). The origin of the peak results mainly from the competition between CO_2 reduction and the hydrogen evolution reaction (HER) or hydrogen absorption (for the layer thicker than 3 ML). The cathodic current rise is observed earlier on the potential scale in the presence of CO_2 because the hydrogen ions reduction is much faster at lower pH's. The carbon dioxide electroreduction starts at −0.1 V, and below this potential, the proton reduction processes are inhibited by adsorbed products of CO_2 electroreduction. Increase of the CO_2 electroreduction rate at lower potentials causes higher surface poisoning, thus resulting in a significant overall current decrease. The further current increase (below −0.5 V) is related to HER process occurring at fully poisoned electrode surface. More details supporting this explanation will be discussed later. It is noteworthy that similar results were observed for CO_2 electroreduction at copper electrodes.[29,30] The potential position of this peak is strongly dependent on the scan rate (see Figure S1 in Supporting Information). In the anodic cycle, the current peaks at 0.80 V for 5 ML and 0.72 V for 10 ML (Figure 4, red lines) are related to hydrogen desorption occurring at the onset of the CO oxidation (as will be later discussed). It should be stressed that total charges of hydrogen desorption, calculated from these peaks, are proportional to the layer thickness (Q = 351 μC cm^{-2} for 5 ML and Q = 849 μC cm^{-2} for 10 ML). Without CO_2 in the solution (Figure 4, black lines) anodic currents are dominated by molecular hydrogen oxidation reaction (HOR).

3.4. CO_2 Electroreduction in Acidic and Neutral Environments at Pd/Au(111). To evaluate the kinetic activity toward CO_2 electroreduction in both acidic and neutral environments, we have recorded cyclic voltammograms after CO_2 reduction performed in the chronoamperometric experiments during time, t_{ad} = 2 s, and for different electroreduction potentials (E_{ad}). The latter has been changed within the range 0.05 to −1.00 V vs RHE. These experiments have been carried out in $KHCO_3$ and $HClO_4$ solutions.

Figure 5 shows voltammograms collected for 5 ML-Pd/Au(111) after the chronoamperometric CO_2 reduction (at

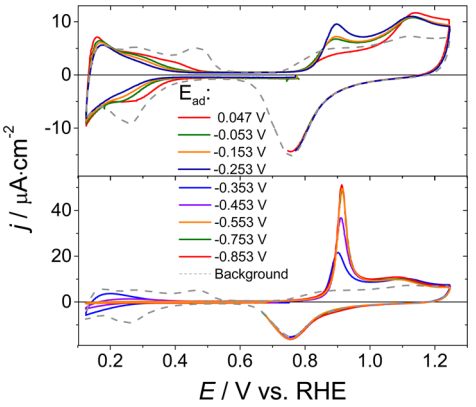

Figure 5. Anodic stripping voltammograms collected for different reduction potentials, E_{ad}, for 5 ML-Pd/Au(111) in 0.1 M $KHCO_3$ CO_2-saturated solution after holding for t_{ad} = 2 s. Scan rate: 10 mV s^{-1}.

different potentials, E_{ad}) in CO_2-saturated 0.1 M potassium bicarbonate. The voltammetric anodic current in the oxide region forms two peaks. The position of these peaks on the potential scale is dependent on the potential E_{ad}. The first peak appearing at 0.890 V for E_{ad} = −0.053 V shifts toward more positive potential with decreasing E_{ad}, up to 0.920 V for E_{ad} = −0.853 V. In the same time the second peak appearing initially at 1.125 V shift toward slightly less negative potentials 1.075 V at E_{ad} = −0.853 V. On the cyclic voltammetry curves, the HUPD currents are markedly suppressed but still visible when E_{ad} > −0.353 V (Figure 5 (Bottom)). At more cathodic electroreduction potentials, E_{ad}, the hydrogen region entirely disappears. As mentioned earlier during discussion of Figure 4 data, the results imply the formation of a poisoning intermediate such as CO strongly bound to the electrode surface.

Similar results were obtained for one Pd monolayer, 1 ML-Pd/Au(111). Figure S3 in the Supporting Information illustrates the anodic stripping voltammograms also recorded in CO_2-saturated 0.1 M $KHCO_3$ for t_{ad} = 2 s at various reduction potentials, E_{ad}. The first anodic peak in the oxide region appear for more negative potentials E_{ad} than previously (for 5 ML-Pd) and also shifts in the opposite direction with decreasing E_{ad}, i.e., toward less negative potentials. The latter effect is most probably related to the increasing number of defects present at the 1 ML-Pd after multiple oxidation/reduction cycles. The second peak related to CO oxidation from palladium terraces and appearing above 1.05 V is also more pronounced for 1 ML-Pd than for thicker palladium deposits. This observation reconfirms our view about the dendric shape characteristic of 5 ML-Pd/Au(111).

dx.doi.org/10.1021/la5025247 | Langmuir 2014, 30, 14314−14321

It is interesting to compare analogous results obtained in the acidic environments (see Figure S2 in the Supporting Information). As previously, these curves are recorded after potentiostatic CO_2 electroreduction performed for t_{ad} = 2 s and for different potentials E_{ad}. After each chronoamperometric experiment, diagnostic cyclic voltammograms have been recorded with the same electrode in the CO_2-saturated 0.1 M $HClO_4$ solution. It is interesting to note that, despite the application of highly cathodic electroreduction potentials (e.g., E_{ad} = −0.88 V), the hydrogen UPD region is still visible. This result clearly shows that, although higher current densities have been observed in the acidic solutions, the overall current efficiency for the CO_2 electroreduction is much higher in neutral solutions.

3.5. Identification of Electroreduction Products. CO Stripping Experiments. CO_2 reduction on Pd catalysts occurs in the hydrogen OPD region, and during this process, intermediate products such as CO are formed. According to Hoshi et al.,[4] CO is the only product of the CO_2 reduction on Pd(111) in acidic solution. To get better insight into the CO adsorption on palladium overlayers, we have conducted CO-stripping experiments as a function of the CO dosing potential, chosen from double layer, HUPD, and HOPD region. However, it should be emphasized that it is not possible to fully reproduce conditions, under which CO_2 undergo electroreduction. For example, if the CO adsorption would be performed in the CO_2 saturated solution, then just after introduction of CO, the pH of the solution would be undefined. Hence, in order to avoid the CO adsorption under imprecise experimental conditions, we have performed CO stripping in 0.1 $KHCO_3$, that is at pH = 8.9. However, it should be remembered that CO_2 reduction takes place at pH = 6.8, and therefore the precise CO oxidation characteristics may differ in both experiments.

For 1 ML-Pd/Au(111) with CO dosed at 0.52 V (Figure 6A, red lines), oxidation (the stripping step) results in the formation of three overlapped peaks; the first one, being sharp and appearing at 0.855 V, characteristic of the CO oxidation from monatomic steps; the second one (at 0.91 V) originates most likely also from a perturbed surface; and the last one, namely the boarder peak at 1.07 V, reflects the oxidation of CO adsorbed on (111) terraces. To date, the CO-stripping experiments have not been reported in neutral solutions; nevertheless, qualitatively similar results were obtained in the acidic solutions for Pd(111) electrode.[8] However, in acidic solutions the current peaks related to CO oxidation are shifted toward positive potentials, which is related to the oxide formation also occurring at higher potentials in acidic media. The influence of pH of the solution on the oxide formation region was visible also at Figure 3. It is noteworthy that in our present experiments (Figure 6) we have observed, additionally, small oxidation currents starting at 0.50 V. These currents are much larger in the case of CO dosed at potentials, 0.129 and −0.02 V (Figure 6A, middle and bottom graphs). It is interesting to note that the CO-dosing potential influences markedly peaks related to CO oxidation from stepped surfaces while the peak current at 1.05 V, that is related to CO oxidation from (111) terraces, is practically unchanged. The total charge characteristic to the oxidation of CO dosed at 0.52 and 0.13 V are the same and equal to Q_{CO} = 220 μC cm^{-2}. Only slightly smaller charge, Q_{CO} = 203 μC cm^{-2}, was observed for oxidation of CO dosed in HOPD region at −0.024 V.

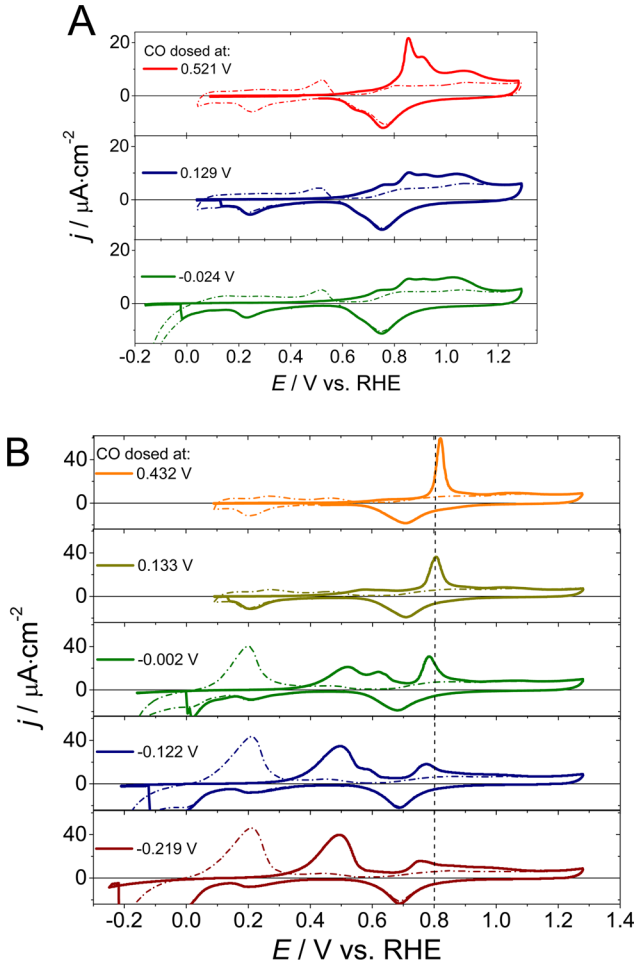

Figure 6. Cyclic voltammograms for CO-stripping (solid lines) and for bare surfaces (dotted lines) on (A) 1 ML-Pd/Au(111) and (B) 5 ML-Pd/Au(111) in CO-free 0.1 M $KHCO_3$. Scan rate: 10 mV s^{-1}. CO was dosed at different potentials for 10 min.

For 5 ML-Pd/Au(111), dosing of CO at 0.43 V (Figure 6B, first graph) results in a sharp CO oxidation peak at 0.82 V characteristic of the stepped or disturbed Pd(111) surface; similar results were reported also for acidic solutions.[8] The potential of CO-oxidation at 5 ML is shifted by 35 mV toward more negative potentials relative to those of 1 ML. This difference between the CO oxidation potentials observed in cases of 1 and 5 ML confirms our view about influence of the Pd layer thickness on the increasing CO binding energy to palladium.[8] We have also considered the CO-stripping experiments for 5 ML-Pd/Au(111) (Figure 6B), in which CO has been dosed at several cathodic potentials. Voltammetric responses are again strongly dependent on CO dosing potential. If CO is dosed at potentials in the hydrogen region, the additional peaks appear within the potential range 0.35–0.65 V. The charge corresponding to CO oxidation in this potential range was estimated to be 110 μC cm^{-2} from the cyclic voltammogram obtained for CO dosing at +0.133 V. For lower dosing potentials significant contribution from the hydrogen absorbed in the palladium bulk appears in this potential range. The charge of the absorbed hydrogen can be estimated by integrating the currents in the hydrogen region recorded for unpoisoned electrode. After correcting for charge related to adsorbed hydrogen $Q_{H,abs} = Q_{H,total} - Q_{H,ad}$ one obtains 480 μC cm^{-2}. This value correspond to the hydrogen

dx.doi.org/10.1021/la5025247 | Langmuir 2014, 30, 14314−14321

concentration n_H/n_{Pd} = 0.43, expressed as a molar ratio, which is below the hydrogen concentration observed for bulk palladium,[12] and it is similar to the hydrogen absorption in palladium nanoparticles.[31] It should be stressed that the hydrogen absorption in the palladium thin layers starts below +0.1 V.[12] The hydrogen desorption from the CO poisoned surface starts at the onset potential for CO oxidation. Total anodic charges obtained in CO stripping experiments were corrected for $Q_{H,abs}$, and these charges were equal to 280 μC cm^{-2} for both CO dosed at −0.122 and −0.219 V. Similar charges were obtained when the CO was adsorbed in the double layer region (at 0.432 V). Hence, it can be concluded that the total CO oxidation charge is basically identical for all experiments with different dosing potentials, which is consistent with the view about inability of CO to undergo reduction in the investigated potential ranges.

3.6. Catalytic Activity for CO_2 Electroreduction. Initial Reaction Rates. The activity toward CO_2 electroreduction has been more quantitatively studied in neutral solutions with the aid of the potential program based on that proposed by Hoshi et al.[32] Each measurement has been started by holding the electrode potential at the double layer potential (E_{dl} = 0.55 V) for 30 s. Then potential has been stepped down to more negative values (E_{ad}), including those where CO_2 reduction proceeds, and the potential has been held for different times (t_{ad}). During the time (t_{ad}), the reduction products have been formed and adsorbed on the electrode surface. The potential has been subsequently stepped back to E_{dl}. Next, the solution has been subjected to purging with CO_2 to remove dissolved hydrogen created during each electroreduction step. After 5 min, the potential has been scanned and the respective voltammogram has been recorded at the 10 mV s^{-1} scan rate. The anodic charge has been related to oxidation of the CO_2 electroreduction products. Carbon dioxide electroreduction initial rate ($v_{t=0}$), defined by eq 1:[32]

$$v_{t=0} = (dQ_{CO}/dt)_{t=0} \quad (1)$$

in which the Q_{CO} values are charges from anodic stripping voltammograms whereas t refers to different adsorption times. Figure S4 in the Supporting Information shows charges measured for 5 ML-Pd/Au(111) as a function of adsorption time. The slope off this relationship gives initial rates, $v_{t=0}$, shown in Figure 7 as a function of potential for 1 and 5 ML deposits.

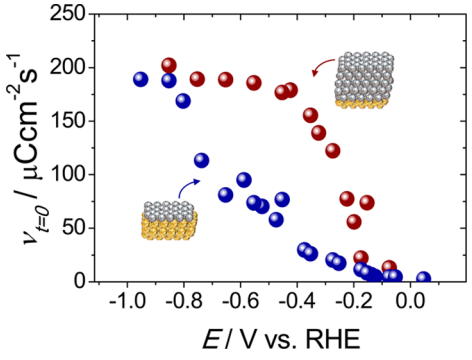

Figure 7. Dependencies of the initial reaction rate, $v_{t=0}$, for CO_2 reduction on potential for 1 ML-Pd/Au(111) and 5 ML-Pd/Au(111). Experiments performed in CO_2-saturated 0.1 M $KHCO_3$.

From Figure 7 it is apparent that higher activity for CO_2 reduction has been observed for the 5 ML-Pd system rather than 1 ML one. While the behavior characteristic of the 5 ML-Pd system resembles that known for Pd(111),[8] it is reasonable to expect that the initial CO_2-reduction rate for the 1 ML-Pd system is affected by the presence of Au(111) substrate and the related lattice strain effects. It should be remembered that, during stripping experiments (Figure 6A), the CO interaction has been found to be weaker on the 1 ML system because the direct influence of Au(111) substrate.

3.7. Copper Underpotential Deposition on 1 and 5 ML Pd/Au(111). To consider multilayered catalytic systems, copper atoms have been underpotentially deposited on palladium overlayers. Figure 8 shows five initial cycles recorded

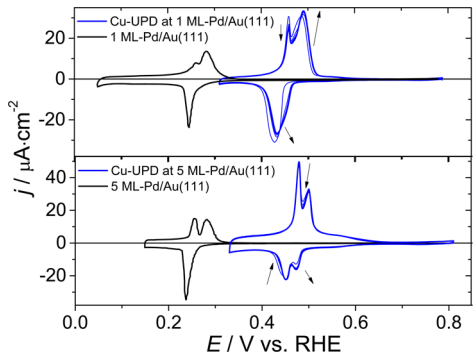

Figure 8. Cyclic voltammograms of 1 ML (top) and 5 ML (bottom) Pd/Au(111) in pure 0.1 M H_2SO_4 (black lines) and in the presence of 4.0 × 10^{-4} M $CuSO_4$ (blue lines). Scan rate: 5 mV s^{-1}.

in voltammetric experiments in the presence of the copper(II) ions (blue lines). Stable response observed already from the second cycle with only minor deviations in the very first one (indicated by the arrows) implies that the deposition does not lead to the formation of a surface alloy but rather the smooth layer of copper atoms is deposited, thus indicating that the palladium overlayers are not damaged by the copper deposition. Interestingly, the copper adsorption/desorption currents characteristic of the Cu-UPD system are qualitatively similar to those known for the behavior of hydrogen in the UPD region (Figure 8, black and blue lines). A single pair of peaks has been observed for Cu-UPD on Pd(111).[33] This suggests that two pairs of peaks observed here for 5 ML-Pd electrode correspond to the electroactivity of copper deposited on the first and the subsequent Pd-layers, as it was previously observed in the case of hydrogen UPD. It is noteworthy that copper deposition at palladium overlayers is an entirely reversible process even at 1 ML-Pd/Au(111), as can be deduced from the charge balance of the deposition/desorption charges. The theoretical value for the Cu-UPD charge, based on assumption about the full copper coverage and the complete copper discharge ($Cu^{2+} + 2e^- = Cu^0$), is 478 μC cm^{-2}.[33] Kolb and co-workers reported that, the charge equal to 400 μC cm^{-2} for Cu-UPD on Pd(111), corresponded to 0.8 of the complete Cu monolayer. In this study, charges consumed during the Cu-UPD on the palladium overlayers are 325 and 337 μC cm^{-2} for 1 and 5 ML-Pd systems, respectively. This result corresponds to the surface coverage by the Cu overlayer being on the order of 0.65 ML.

To perform deposition of copper on 1 ML-Cu level, the potential has been scanned at 5 mV s^{-1} from the open circuit

dx.doi.org/10.1021/la5025247 | Langmuir 2014, 30, 14314−14321

potential down to 0.31 V and, subsequently, held for 100 s. Then, the electrode has been transferred to the 0.1 M potassium bicarbonate solution under the inert argon atmosphere. Cyclic voltammograms characteristic of the freshly deposited 1 ML-Cu on 1 ML-Pd/Au(111) (marked as 1 ML-Cu/1 ML-Pd/Au(111)) and on 5 ML-Pd/Au(111) (marked as 1 ML-Cu/5 ML-Pd/Au(111)) are shown in Figure 9. For both

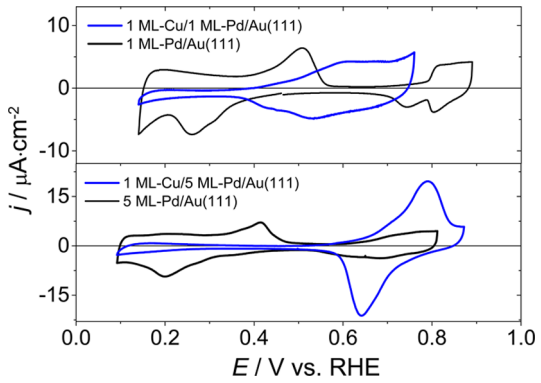

Figure 9. Cyclic voltammograms for 1 ML-Cu covered 1 ML-Pd/Au(111) (top) and 5 ML-Pd/Au(111) (bottom) recorded in CO_2-free 0.1 M $KHCO_3$ (blue lines). For comparison, the responses for 1 ML (top) and 5 ML (bottom) Pd/Au(111) are also shown (black lines). Scan rate: 10 mV s^{-1}.

1 ML-Pd and 5 ML-Pd systems covered with 1 ML-Cu, the hydrogen peaks are absent, thus indicating suppression of the hydrogen UPD. A new pair of broad peaks related to copper oxidation has appeared at higher potentials. After prolonged cycling in bicarbonate solution, the copper monolayer can be entirely removed from the electrode surface. This process is much faster in the CO_2-saturated solution and leads to the gradual disappearance of the Cu oxidation peaks followed by the reconstruction of H-UPD region (not shown here).

The carbon dioxide electroreduction on Cu-UPD-covered multilayered catalysts is shown in Figure 10A. Although all electrodes have the outermost layers in a form of copper monolayer, the strong background effects have led to significantly different voltammetric behaviors. Indeed, the carbon dioxide reduction starts at significantly less negative potentials for 1 ML-Cu/1 ML-Pd/Au(111) and 1 ML-Cu/5 ML-Pd/Au(111) in comparison to the Pd-free system of 1 ML-Cu/Au(111). Apparently, the surface is the most poisoned by the reaction intermediate (mostly CO) in the case of 5 ML-Pd because the lowest cathodic current densities are observed for this electrode. In the case of 1 ML-Cu/Au(111) electrode, the CO_2 electroreduction potentials are the most negative, but much weaker poisoning is expected because both cathodic and anodic voltammetric scans largely overlap. An intermediate behavior was observed for 1 ML-Cu/1 ML-Pd/Au(111) electrode. This catalyst surface is markedly less poisoned than the electrode utilizing 5 ML-Pd, which has manifested in terms of both higher cathodic current density and smaller discrepancy between cathodic and anodic responses (Figure 10A). UPD deposition of copper monolayer on 1 and 5 ML palladium deposit leads to the formation of multilayered catalyst structure, the electronic properties of which can be easily tuned by deposition different Cu coverage or by changing the thickness of the Pd underneath layer. Figure 10B shows the comparison of all investigated catalysts. From inspection of this Figure it is reasonable to expect that the catalytic performance of the

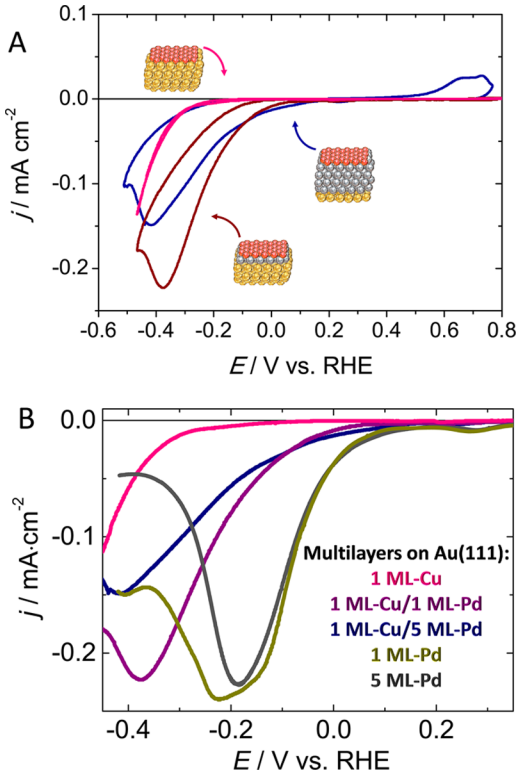

Figure 10. (A) Cyclic voltammograms of 1 ML-Cu/5 ML-Pd/Au(111) (blue line), 1 ML-Cu/1 ML-Pd/Au(111) (violet line), and the system without Pd layer, 1 ML-Cu/Au(111) (pink line) recorded in CO_2-saturated 0.1 M $KHCO_3$. Scan rate: 10 mV s^{-1}. (B) Comparison of all investigated catalysts; cathodic scan at 10 mV s^{-1}.

multilayered systems would be further tuned by deposition of submonolayer amounts of both Pd and Cu. Further research is along this line.

4. CONCLUSIONS

We have address here the advanced synthetic routes and comprehensive characterization of model multilayered catalysts composed of monatomic layer of copper covering palladium overlayers (0.8−10 ML) deposited on the well-defined Au(111) surface. The catalysts have been designed for CO_2 electroreduction reaction. All measurements have been conducted with well-defined Pd deposits initially characterized in pure sulfuric and/or perchloric acid solutions. Hydrogen UPD charges have been found to be ca. 10% lower in the presence of CO_2, thus indicating a weak specific adsorption of CO_2 at the Pd surface. The main product of the CO_2 electroreduction at Pd pseudomorphic layers is carbon monoxide. This product has been confirmed by CO stripping experiments. In the latter case, the CO oxidation charge is virtually independent of the CO adsorption potential, which suggests that CO does not undergo further electroreduction in the investigated range of potentials. Thickness of the monatomic layers of Pd deposited on well-defined Au(111) surfaces influences their activity toward CO_2 electroreduction. The initial rate of CO formation is greater for thicker deposits.

Deposition of monatomic layer of copper is a reversible process on palladium pseudomorphic layers, thus implying that the obtained catalysts have truly layered structure on the atomic scale. The catalytic activity of the outermost Cu monolayer toward CO_2 electroreduction is strongly dependent on the

dx.doi.org/10.1021/la5025247 | Langmuir 2014, 30, 14314−14321

support. By deliberate controlling the affinity for CO adsorption, the apparent catalytic activity toward formation of CO poisoning intermediate (during CO_2 reduction) has been tuned to decrease systematically in the following order: Pd(111) > 5 ML-Pd > 1 ML-Pd > 1 ML-Cu/5 ML-Pd > 1 ML-Cu/1 ML-Pd > 1 ML Cu. This result points out the possibility of tuning catalytic properties by designing multilayered structures obtained by sequential UPD strategies.

■ ASSOCIATED CONTENT

Supporting Information

Figures S1−S4. This material is available free of charge via the Internet at http://pubs.acs.org.

■ AUTHOR INFORMATION

Corresponding Authors

*E-mail rafjur@chem.uw.edu.pl (R.J.).
*E-mail pkulesza@chem.uw.edu.pl (P.J.K.).

Notes

The authors declare no competing financial interest.

■ ACKNOWLEDGMENTS

This work was supported by National Research Centre, Poland (Project # 2011/03/B/ST4/02409).

■ REFERENCES

(1) Jitaru, M.; Lowy, D. A.; Toma, M.; Toma, B. C.; Oniciu, L. Electrochemical Reduction of Carbon Dioxide on Flat Metallic Cathodes. *J. Appl. Electrochem.* **1997**, *27*, 875−889.

(2) Hansen, H. A.; Varley, J. B.; Peterson, A. A.; Nørskov, J. K. Understanding Trends in the Electrocatalytic Activity of Metals and Enzymes for CO_2 Reduction to CO. *J. Phys. Chem. Lett.* **2013**, *4*, 388−392.

(3) Kibler, L. A.; El-Aziz, A. M.; Hoyer, R.; Kolb, D. M. Tuning Reaction Rates by Lateral Strain in a Palladium Monolayer. *Angew. Chem., Int. Ed.* **2005**, *44*, 2080−2084.

(4) Hoshi, N.; Noma, M.; Suzuki, T.; Hori, Y. Structural Effect on the Rate of CO_2 Reduction on Single Crystal Electrodes of Palladium. *J. Electroanal. Chem.* **1997**, *421*, 15−18.

(5) Steidtner, J.; Hernandez, F.; Baltruschat, H. Electrocatalytic Reactivity of Pd Monolayers and Monatomic Chains on Au. *J. Phys. Chem. C* **2007**, *111*, 12320−12327.

(6) Vidal-Iglesias, F. J.; Solla-Gullon, J.; Herrero, E.; Aldaz, A.; Feliu, J. M. Pd Adatom Decorated (100) Preferentially Oriented Pt Nanoparticles for Formic Acid Electrooxidation. *Angew. Chem., Int. Ed.* **2010**, *49*, 6998−7001.

(7) Herrero, E.; Buller, L. J.; Abruna, H. D. Underpotential Deposition at Single Crystal Surfaces of Au, Pt, Ag and Other Materials. *Chem. Rev.* **2001**, *101*, 1897−1930.

(8) El-Aziz, A. M.; Kibler, L. A. Influence of Steps on the Electrochemical Oxidation of Co Adlayers on Pd(111) and on Pd Films Electrodeposited onto Au(111). *J. Electroanal. Chem.* **2002**, *534*, 107−114.

(9) Duncan, H.; Lasia, A. Hydrogen Adsorption/Absorption on Pd/Pt(111) Multilayers. *J. Electroanal. Chem.* **2008**, *621*, 62−68.

(10) Tang, J.; Petri, M.; Kibler, L. A.; Kolb, D. M. Pd Deposition onto Au(111) Electrodes from Sulphuric Acid Solution. *Electrochim. Acta* **2005**, *51*, 125−132.

(11) Hara, M.; Linke, U.; Wandlowski, T. Preparation and Electrochemical Characterization of Palladium Single Crystal Electrodes in 0.1 M H_2SO_4 and $HClO_4$. Part I. Low-Index Phases. *Electrochim. Acta* **2007**, *52*, 5733−5748.

(12) Duncan, H.; Lasia, A. Separation of Hydrogen Adsorption and Absorption on Pd Thin Films. *Electrochim. Acta* **2008**, *53*, 6845−6850.

(13) Kibler, L. A. Dependence of Electrocatalytic Activity on Film Thickness for the Hydrogen Evolution Reaction of Pd Overlayers on Au(111). *Electrochim. Acta* **2008**, *53*, 6824−6828.

(14) Kibler, L. A.; El-Aziz, A. M.; Kolb, D. M. Electrochemical Behaviour of Pseudomorphic Overlayers: Pd on Au(111). *J. Mol. Catal. A: Chem.* **2003**, *199*, 57−63.

(15) Naohara, H.; Ye, S.; Uosaki, K. Thickness Dependent Electrochemical Reactivity of Epitaxially Electrodeposited Palladium Thin Layers on Au(111) and Au(100) Surfaces. *J. Electroanal. Chem.* **2001**, *500*, 435−445.

(16) Obradovic, M. D.; Gojkovic, S. L. HCOOH Oxidation on Thin Pd Layers on Au: Self-Poisoning by the Subsequent Reaction of the Reaction Product. *Electrochim. Acta* **2013**, *88*, 384−389.

(17) Hansgen, D. A.; Vlachos, D. G.; Chen, J. G. Using First Principles to Predict Bimetallic Catalysts for the Ammonia Decomposition Reaction. *Nat. Chem.* **2010**, *2*, 484−489.

(18) Ragoisha, G.; Bondarenko, A.; Osipovich, N.; Rabchynski, S.; Streltsov, E. Multiparametric Characterisation of Metal-Chalcogen Atomic Multilayer Assembly by Potentiodynamic Electrochemical Impedance Spectroscopy. *Electrochim. Acta* **2008**, *53*, 3879−3888.

(19) Varela, A. S.; Schlaup, C.; Jovanov, Z. P.; Malacrida, P.; Horch, S.; Stephens, I. E. L.; Chorkendorff, I. Co2 Electroreduction on Well-Defined Bimetallic Surfaces: Cu over Layers on Pt(111) and Pt(211). *J. Phys. Chem. C* **2013**, *117*, 20500−20508.

(20) Stevens, G. B.; Reda, T.; Raguse, B. Energy Storage by the Electrochemical Reduction of CO_2 to CO at a Porous Au Film. *J. Electroanal. Chem.* **2002**, *526*, 125−133.

(21) El-Aziz, A. M.; Kibler, L. A.; Kolb, D. M. The Potentials of Zero Charge of Pd(111) and Thin Pd Overlayers on Au(111). *Electrochem. Commun.* **2002**, *4*, 535−539.

(22) Alvarez, B.; Climent, V.; Feliu, J. M.; Aldaz, A. Determination of Different Local Potentials of Zero Charge of a Pd-Au(111) Heterogeneous Surface. *Electrochem. Commun.* **2000**, *2*, 427−430.

(23) Herrero, E.; Feliu, J. M.; Wieckowski, A.; Clavilier, J. The Unusual Adsorption States of Pt(111) Electrodes Studied by an Iodine Displacement Method - Comparison with Au(111) Electrodes. *Surf. Sci.* **1995**, *325*, 131−138.

(24) Duncan, H.; Lasia, A. Mechanism of Hydrogen Adsorption/Absorption at Thin Pd Layers on Au(111). *Electrochim. Acta* **2007**, *52*, 6195−6205.

(25) Lebouin, C.; Olivier, Y. S.; Sibert, E.; Millet, P.; Maret, M.; Faure, R. Electrochemically Elaborated Palladium Nanofilms on Pt(111): Characterization and Hydrogen Insertion Study. *J. Electroanal. Chem.* **2009**, *626*, 59−65.

(26) Martin, M. H.; Lasia, A. Hydrogen Sorption in Pd Monolayers in Alkaline Solution. *Electrochim. Acta* **2009**, *54*, 5292−5299.

(27) Butler, J. N. *Carbon Dioxide Equilibria and Their Applications*; CRC Press: Boca Raton, FL, 1991.

(28) Tripković, A.; Popović, K.; Momčilović, J.; Dražić, D. Kinetic and Mechanistic Study of Methanol Oxidation on a Pt (110) Surface in Alkaline Media. *Electrochim. Acta* **1998**, *44*, 1135−1145.

(29) Hori, Y.; Murata, A.; Takahashi, R. Formation of Hydrocarbons in the Electrochemical Reduction of Carbon-Dioxide at a Copper Electrode in Aqueous-Solution. *J. Chem. Soc., Faraday Trans. 1* **1989**, *85*, 2309−2326.

(30) Hara, K.; Tsuneto, A.; Kudo, A.; Sakata, T. Change in the Product Selectivity for the Electrochemical CO_2 Reduction by Adsorption of Sulfide Ion on Metal Electrodes. *J. Electroanal. Chem.* **1997**, *434*, 239−243.

(31) Yamauchi, M.; Kitagawa, H. Hydrogen Absorption of the Polymer-Coated Pd Nanoparticle. *Synth. Met.* **2005**, *153*, 353−356.

(32) Hoshi, N.; Suzuki, T.; Hori, Y. Step Density Dependence of CO_2 Reduction Rate on Pt(S)-[N(111)X(111)] Single Crystal Electrodes. *Electrochim. Acta* **1996**, *41*, 1647−1653.

(33) Okada, J.; Inukai, J.; Itaya, K. Underpotential and Bulk Deposition of Copper on Pd(111) in Sulfuric Acid Solution Studied by in Situ Scanning Tunneling Microscopy. *Phys. Chem. Chem. Phys.* **2001**, *3*, 3297−3302.